



An Experimental Study of High-Damping Rubber Bearings (HDRB) and Their Implications for the Seismic Performance of Cable-Stayed Bridges

Ahmed Ramadan Ahmed^{1,*}, Yermoshin N. A², Feras A. R. Temimi³

1. Department of Civil Engineering, Faculty of Engineering, Peter the Great St. Petersburg Polytechnic University, Saint-Petersburg, 195251, Russia^{1,*}
engahmedramadan103@gmail.com^{1,*}

2. Department of Civil Engineering, Faculty of Engineering, Peter the Great St. Petersburg Polytechnic University, Saint-Petersburg, 195251, Russia²
ermonata@mail.ru²

3. Department of Civil Engineering, Faculty of Engineering, Peter the Great St. Petersburg Polytechnic University, Saint-Petersburg, 195251, Russia³
altemimi.f@edu.spbstu.ru³
Faculty of Engineering, University of Thi-Qar, Iraq³
feras.temimi@utq.edu.iq³

Correspondence Author*:

Ahmed Ramadan Ahmed

engahmedramadan103@gmail.com

Abstract

This article investigates the efficiency of high damping rubber bearings (HDRB), which are made of special rubber with excellent damping attributes and layers of steel. HDRB isolators have excellent flexibility, vibration reduction ability, and high restoring ability for controlling the seismic response of long-span cable-stayed bridge systems under near-fault ground motions. The seismic isolation of cable-stayed bridges is achieved using high-damping rubber bearings (HDRB). High-damping rubber bearings have excellent seismic effects during earthquakes. The elastic stiffness of the bearing depends on the degree of deformation. When the deformation is small, the stiffness will be large. Therefore, compressive stiffness is one of the key parameters in the design of seismic isolation bearings for cable-stayed bridges. For this reason, predicting the behavior of high-damping rubber bearings under compressive loads is highly important for their design. Therefore, the experimental verification of high-damping rubber bearings (HDRB) for compressive loading was tested according to the standard assumptions in STN EN 1337-3. Firstly, periodic vertical compression tests are performed, and the high damping rubber (HDRB) capabilities and energy dissipation are analysed, taking into account the effect of vertical compression and loading frequency. Secondly, a corrected calculation of the vertical stiffness for high-damping rubber bearings is proposed based on experimental data to provide a more accurate and realistic tool for measuring the vertical



mechanical properties of rubber bearings. The test results prove that HDRB has the most advanced performance. For the fatigue property, the hysteresis curves of the HDRB plump both vertically, which provides a good energy dissipation effect.

Keywords: high-damping rubber bearing (HDRB), seismic isolation, cable-stayed bridge, seismic response, earthquake, experiment, STN EN 1337-3, compression test.

Introduction

In the last few decades, cable-stayed bridges have become popular structures throughout the world due to their appealing aesthetics, full and efficient use of structural materials, fast construction, and increased stiffness compared to suspension bridges (Casciati et al., 2008; Ren and Obata, 1999). The design and construction technologies for cable-stayed bridges are also making rapid progress. The central span of cable-stayed bridges, such as the Russky Island cable-stayed bridge (1104 m) in Russia, has exceeded 1000 m (Ahmed, A. R., & Ermoshin, N. 2022). These bridges are critical lifeline facilities of local and national transportation systems. Some of them have been built in high seismic zones, and the seismic safety of such huge structures is of great concern (Chang et al., 2004).

A number of studies have focused on the seismic behavior of cable-stayed bridges under extreme dynamic loads (Ali and Abdel-Ghaffar, 1994; Li et al., 2011; Martí'nez-Rodrigo and Filiatrault, 2015; Shrestha, 2015; Wang et al., 2015). These studies have shown that the performance of a cable-stayed bridge depends on the mechanism by which the deck is connected to the towers. If the main deck is restrained longitudinally to the tower, it will result in reduced movement under earthquakes but will cause a significant increase in the demands on the towers in terms of bending moment and shear force (Li, S. et al., 2018).

Elastic supports are often used to restrain the displacement of the main deck due to an earthquake. They do not have the ability to dissipate any energy induced by the earthquake. Hence, supplementary damping devices should be introduced to improve the seismic performance of bridge systems. Considering the poor energy-dissipating capacity of elastic supports, supplementary damping devices are often used to add damping to improve the seismic performance of cable-stayed bridges. The earthquake engineering community faces new challenges in seeking and developing new damping technologies that could control the seismic response of cable-stayed bridges (Gu, Z., et al., 2021).

High-damping rubber bearings, also known as HDRB or HDRB isolators, are a kind of seismic isolation bearing similar to lead rubber bearings. Made from special rubber with excellent damping attributes and layers of steel, the HDRB isolators have excellent flexibility, vibration reduction ability, and high restoring ability. Thus, it is an important component of the seismic isolation system and can effectively reduce the damage to bridges and buildings caused by earthquakes. The high-damping rubber bearing itself performs the isolation function and does not need to configure other devices, so the maintenance and management costs are low. HDR bearing pad is composed of specialized rubber with high damping performance,

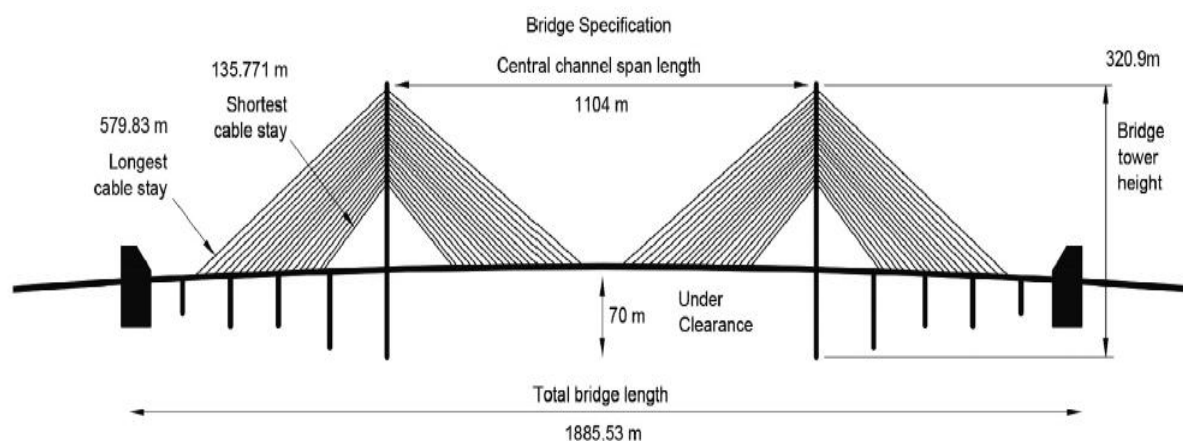


sandwiched together with steel plate layer. When installing, the high-damping rubber bearing is commonly used with top and bottom steel plates and connection accessories.

Cable-stayed bridge

Bridge description. The bridge model used in this study is the Russky Bridge located in Vladivostok, Russia. This bridge is the longest cable-stayed bridge in the world, with a central length of 1,104 meters. The bridge also has the second tallest towers after Millau Bridge and the longest cable (Ahmed, A. R., & Ermoshin, N. 2022). The bridge consists of two A-shaped towers with a height of 319 m, double-level semi-fan configuration cables (total of 168 cable members, The longest cable length: 579.83 m, The shortest cable length: 135.771 m.), a streamlined flat steel box girder having a width of 25.96 m and deck depth: 3.2 m, one transition pier and two auxiliary piers in each side span, carriageway width: 23.8 m, Number of lanes: 4 (two in each direction), The dimensions of the bridge in four lanes with a median of 3 m and road shoulder on 1.5 m make 21 m ($1.5 + (2 \times 3.75) + (1 + 1 + 1) + (2 \times 3.75) + 1.5$), operating lanes 0.75 m wide. The cable members are spaced 2 meters apart at the top of the tower and equidistant 24 meters apart at deck level on the side as well as main spans, all cables are regularly spaced (24 and 12 m apart) along the deck. The bridge configuration is shown schematically in Figure 1 (Ahmed, A. R., & Yermoshin, N. A. 2024; Pipinato, A. 2016).

The aim of this study is to investigate the effectiveness of high-damping rubber bearings (HDRB) for a cable-stayed bridge system. Hence, the isolated system present in the built bridge was not considered in this study.



(a)

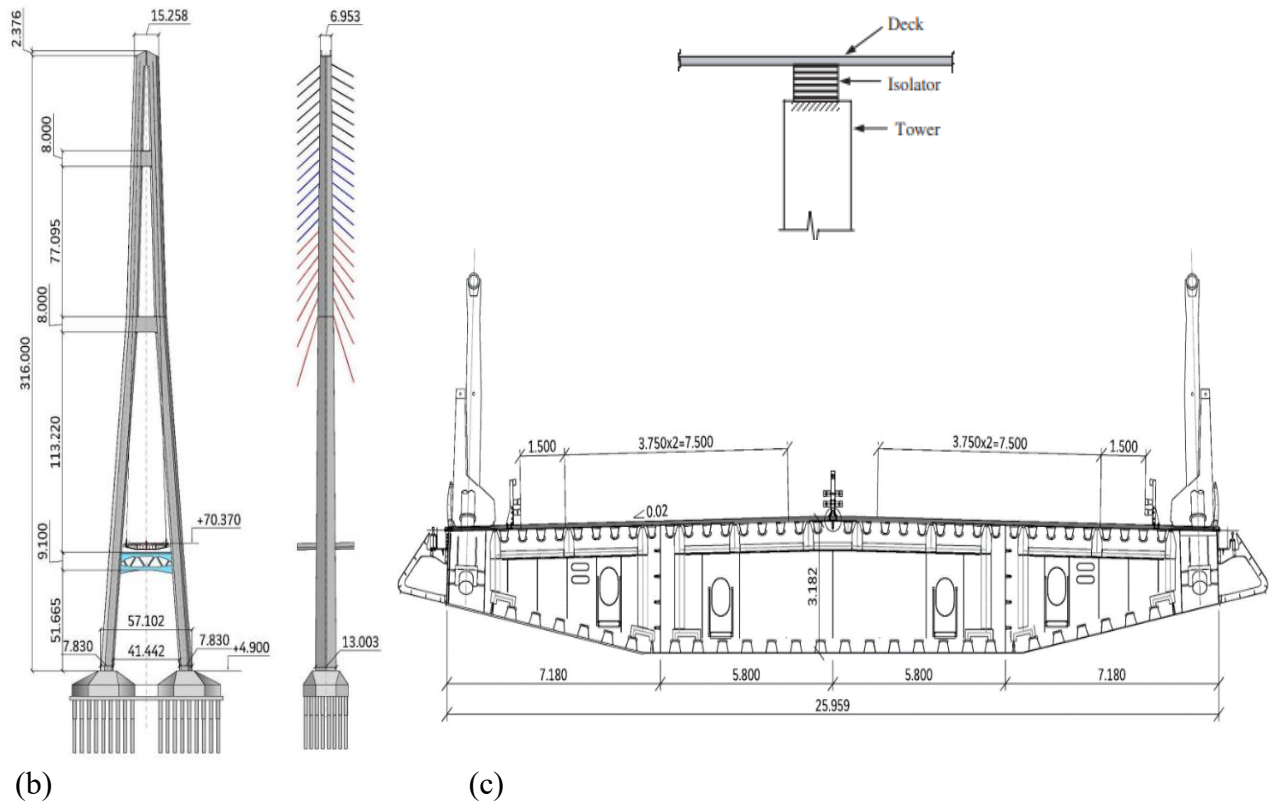


Figure 1. Detailed configuration of the Russky Bridge (meters): (a) longitudinal view of the bridge, (b) transverse views of the towers, and (c) transverse section of the deck (Ahmed, A. R., & Yermoshin, N. A. 2024)

The dead load includes the weights of the cables, girders, floor system, and other parts of the Russky Bridge itself. The cables and girders weights are calculated using an iterative process, and the exact values are taken into account, as mentioned in Table 1. To represent dead loads and the weight of steel structural elements, a longitudinal deck load of 230 kN/m was applied. The parallel strand stays cables had an ultimate tensile strength of 1860 MPa, a modulus of elasticity of $E = 205$ GPa, a design stress of $f_{cbd} = 800$ MPa, and a weight density of $\gamma_{cb} = 84$ kN/m³. The information was taken from the original project. live load is 75 kN/m. The floor system is supposed to be asphalt concrete; 0.20 m thick. In addition, the weight of the other parts of the bridge is considered to be 6 kN/m. The applicable load calculation is given below. The relevant properties of the bridge deck and towers are given in Table 1, and the properties of the cables are given in Table 2 (Ahmed, A. R., & Ermoshin, N. 2022; Pipinato, A. 2016).

Table 1. Weights of the elements of the Russky bridge.



main bridge	structural steel (t)	concrete volume (m ³)	prestressing steel (t)	reinforcing steel (t)	steel for cable-stays (t)
deck of main span	22567				
deck of side spans		80490	647	8792	
piers		80490		8792	
pylons	3394	41419	133	10462	
stay cables					3650

Distributed load = $3(9 + 2.5 + 2.5 + 2.5) = 49.5 \frac{\text{kN}}{\text{m}}$

Concentrated load (double axel) = $300+200+100+0 = 600 \text{ kN}$

Floor system and other parts of the bridge = $66 \frac{\text{kN}}{\text{m}}$

Table 2.Properties for the stay cables of the cable-stayed bridge.

cable number	Area (m2)	Diameter (m)	cable number	Area (m2)	Diameter (m)
1	0.17971	0.478466	12	0.04505	0.239571
2	0.16615	0.460067	13	0.03506	0.211331
3	0.15278	0.441157	14	0.02563	0.180688
4	0.13959	0.421689	15	0.01679	0.146237
5	0.12662	0.401625	16	0.01419	0.134426
6	0.11389	0.3809	17	0.01177	0.122443
7	0.10156	0.359689	18	0.00954	0.110239
8	0.08951	0.337669	19	0.00751	0.097821
9	0.07786	0.314933	20	0.00572	0.085376
10	0.06645	0.290942	21	0.00455	0.076169
11	0.05551	0.265919			

As shown in Figure 2, the longitudinal thermal movements and seismic behavior of the Russky Bridge, 1.03 m at each joint. The deck is longitudinally free (no fixed point), centered by the stays and braked by longitudinal dampers at the abutments. For seismic behavior, the maximum displacement is 5 cm longitudinally, 15 cm transversely. Its high flexibility makes the bridge insensitive to earthquakes.

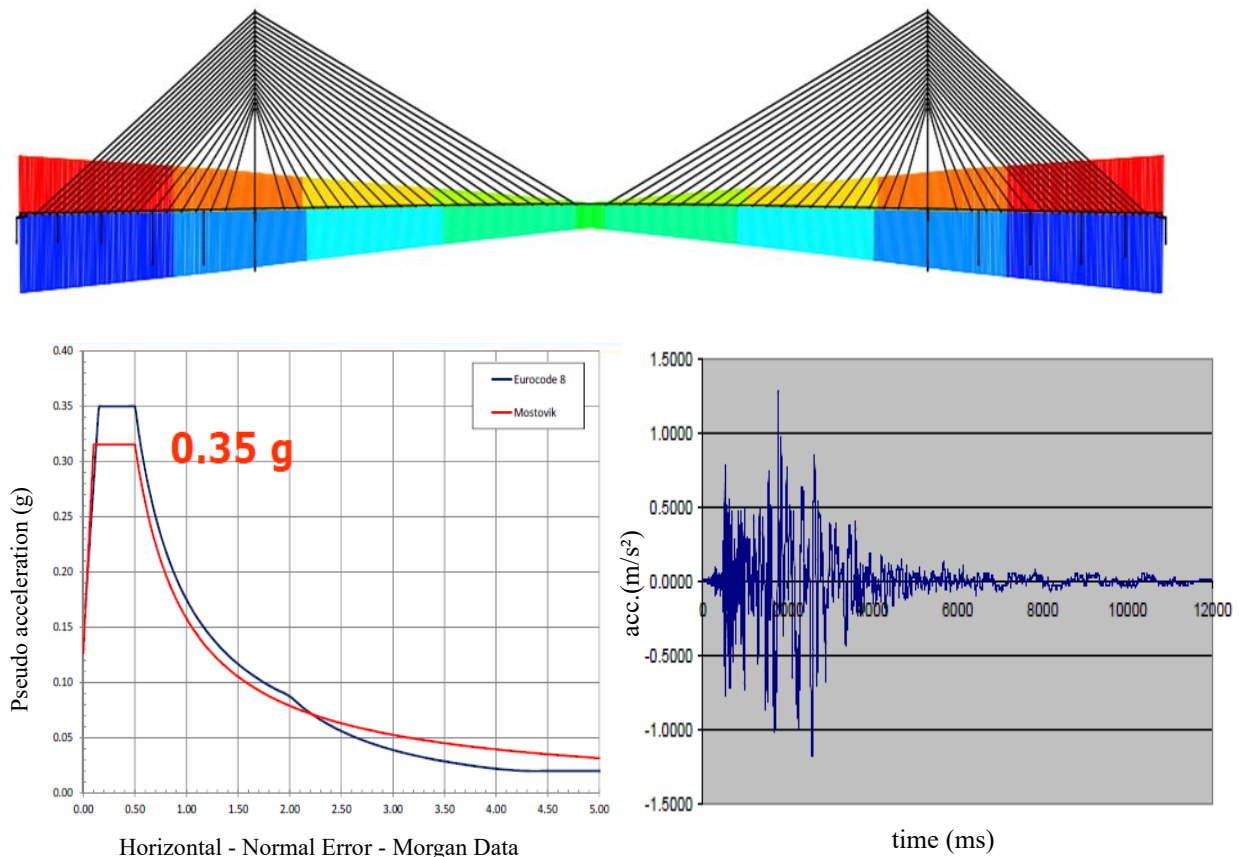


Figure 2. longitudinal thermal movements and seismic behavior of the Russky Bridge.

High damping rubber bearing (HDR)

Figure (3a) depicts the HDRB, which is made up of alternately layered steel and rubber plates. Internal steel shims, often known as shims, provide significantly more stiffness. Steel shims prevent rubber bulging and increase stiffness, but they have no effect on stiffness, which is determined by the elastomer's low shear modulus. The HDRB system's key feature is the combination of spring and viscous damping. Damping inside the bearing can be improved by incorporating fine carbon blocks, oils, resins, and other unique fillers. Figure (3b) depicts the bearing's force deformation characteristics as well as its mathematical model. The restoring force in the bearing, F_b , is calculated as: (Soneji, B. B., & Jangid, R. S. 2006)

$$F_b = c_b \dot{x}_b + k_b x_b, \quad (1)$$

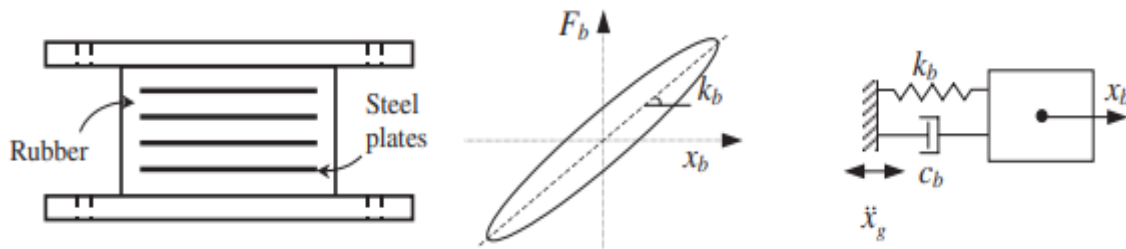
where c_b and k_b are the HDRB system's damping and stiffness coefficients, respectively. The HDRB system's stiffness and damping coefficients are chosen to match the needed values for the isolation time period (T_b) and damping ratio (ξ_b), as described in:



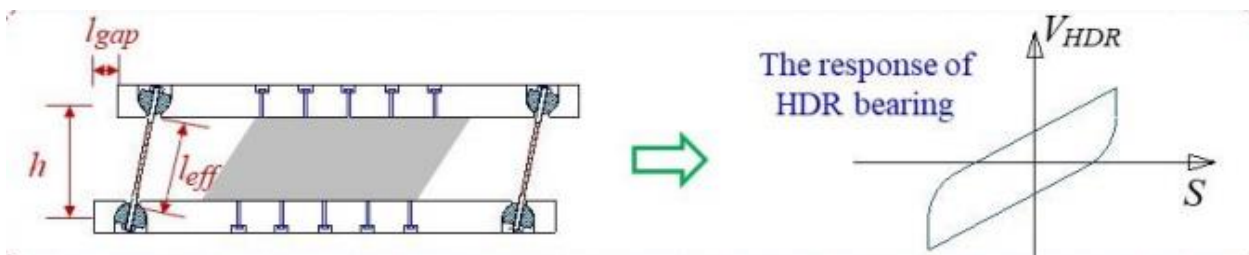
$$T_b = 2\pi \sqrt{\frac{m_d}{\sum k_b}} \quad (2)$$

$$\xi_b = \frac{\sum c_b}{2m_d \omega_b}, \quad (3)$$

The isolation frequency of the bearing system is denoted by $\omega_b = 2\pi / T_b$, while m_d represents the deck's total mass.



(a)



(b)

Figure 3. High damping rubber bearing HDRB insulation system with force deformation behavior and mathematical models (Soneji, B. B., & Jangid, R. S. 2006; Fang, C., et al., 2022).

Working principle of high damping rubber bearing.

By producing large deformation and small rigidity, the high damping rubber bearing has excellent seismic effect during the earthquake. As the elastic stiffness of the bearing depends on its deformation degree. When the deformation is small, the stiffness will be large. The high damping rubber bearing has excellent seismic isolation function by this principle.

During earthquake, the vibration from various directions will impact fixed base building and results in deformation and building or bridge damages. The high damping bearing pad is improved through high damping material, which the damping ratio can approach to 15% to 18%.

Characteristics of HDRB isolators

- The hysteretic characteristic (load deformation curve) of high damping rubber bearing is full, which can play an isolation effect for wind vibration and large, medium and small earthquakes.



- The high damping rubber bearing itself performs the isolation function and does not need to configure other devices, so the maintenance and management cost is low.
- After a large earthquake, the high damping rubber bearing will not produce residual deformation, and the characteristic change is very small, so it does not need to be replaced.
- The elastic properties and damping properties of high damping rubber bearings have little dependence on temperature, that is, they are less affected by temperature, so they are suitable for a wide range of fields.
- The internal EPDM rubber is completely protected which is resistant to the ozone and ultraviolet, so it has better aging-resistant ability.
- HDR high damping rubber has the same superior creep performance as natural rubber.

Experimental Process

Specimen Design

Performing compression tests for HDRB high damping rubber bearings with dimensions (350 x 450 x 105 mm). Information about the rubber and steel layers is as follows: 7 internal steel plates each with a thickness of 4 mm, 2 external rubber layers each with a thickness of 2.5 mm, and 6 internal rubber layers each with a thickness of 12 mm, according to the British Standard "EN 1337-3". Figure 4 and Tab. 3 display the HDRB configuration, which was designed for experimental verification.

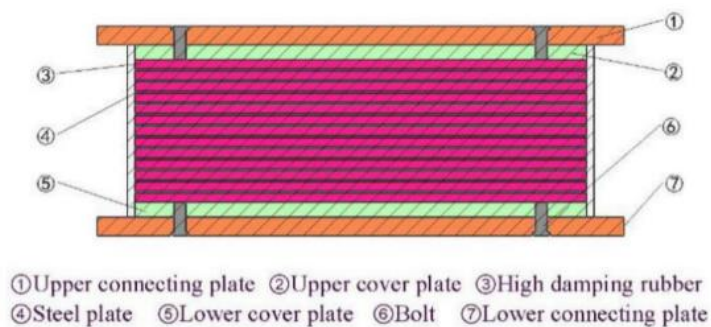


Figure 4. The configuration of HDRB.

Tab. 3: Numbering of bearing, dimensions and number and thickness of layers

Bearing size	a	b	H	n_r	t_i	n_s	t_s
350 × 450 × 105	350	450	105	6	12	7	4

where:

t_i : the thickness of individual layer of elastomer,

n_r : number of layers of elastomer,

t_s : the thickness of inner reinforcing plate,

n_s : number of layers of inner reinforcing plate.

Testing methods



The test machine shall be capable of compressing the bearing under controlled conditions. It shall also provide a method of measuring the compressive load and the compressive deflection to an accuracy of less than or equal 2 % of the maximum values recorded. The platens shall be thick enough to prevent significant distortion (<1 % of measured bearing deflection) under the maximum loading and their dimensions in plan shall be greater than the plan area of the sample under test.

Both the vertical shortening and horizontal displacement were determined using LVDTs with accuracy of 1/100 mm and a range of 150 mm. The LVDTs were fixed horizontally and vertically, as shown in Figure 5, to determine their respective displacements. The vertical displacements were measured using 4 LVDTs at the corners of the loading plates, and the horizontal displacements were measured by 2 LVDTs, as shown in Figure 5.

Test pieces

The test piece shall meet the non-buckling requirement of 5.3.3.7. The average initial thickness of the test piece shall be measured using a minimum of two gauges placed equidistant from the centre of the bearing and on a line passing through the centre of the bearing. An additional pair of gauges may be used in order to establish the variation in thickness across the bearing, and in this case, the gauges shall be arranged symmetrically either at the corners or at the midpoints of the sides. The plan dimensions shall be measured along the edges, but the effective area, A' , of a laminated bearing is given by the area of the plates, not the superficial area of the bearing. The period between vulcanisation and test shall be a minimum of 24 h at the ambient temperature of the laboratory.

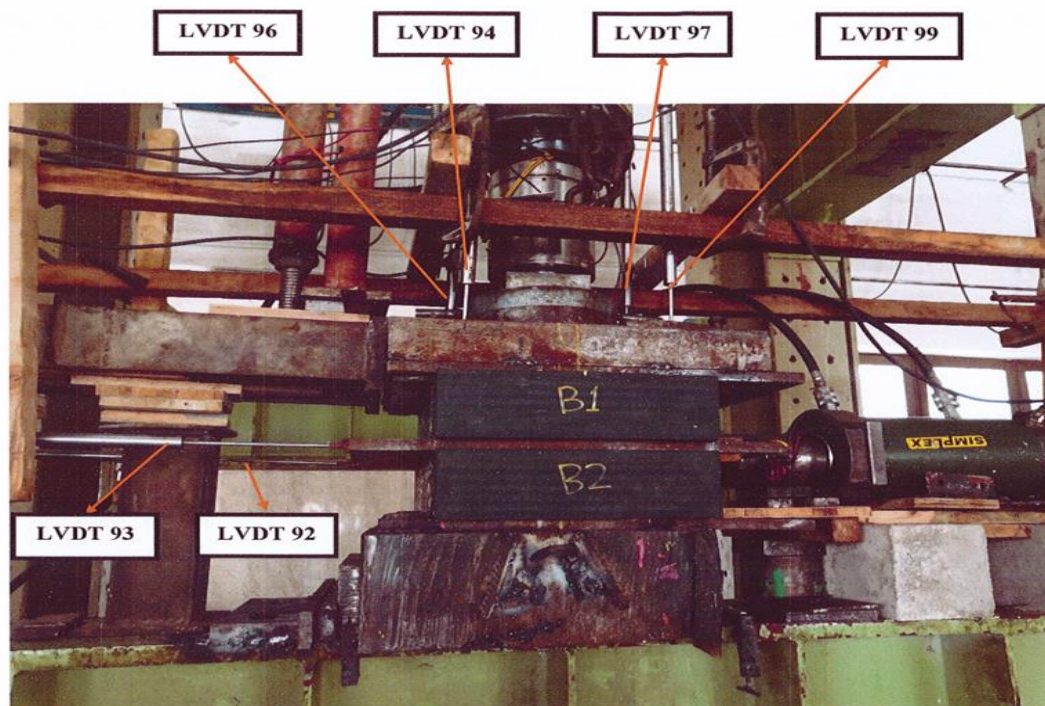


Figure 5: Vertical and Horizontal Displacement Measuring Instruments.

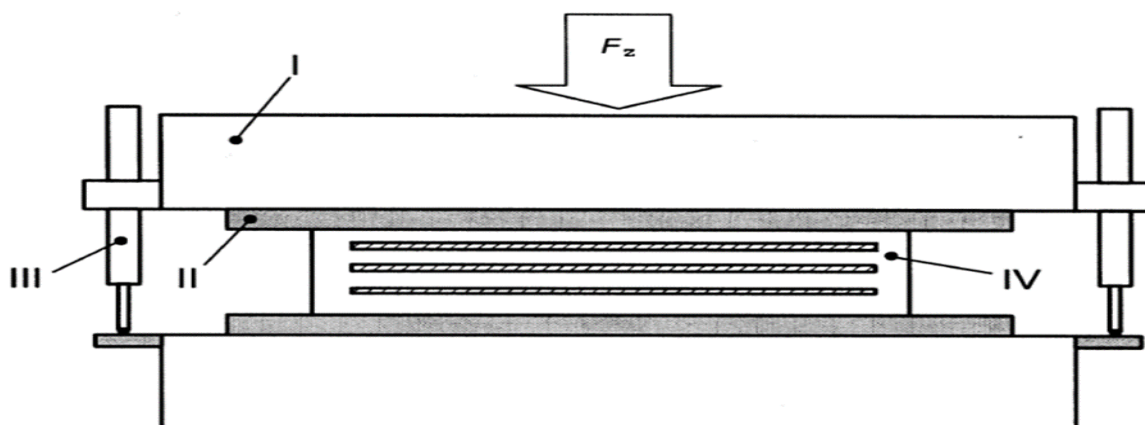


Compression Test

The test consists of measuring the compression of an elastomeric bearing when subjected to increasing compressive loads. From these measurements, the intersecting compression modulus E is calculated, and the surface of the bearing, when under full load, is examined for defects.

The test piece shall be placed at the centre of the testing platen, to an accuracy of better than $1/50$ th of the smaller plan dimension of the test piece. The test was performed as per the British Standards' specifications (BS EN 1337) as follows:

- 1- Setup of the testing machine and the bearing plates as shown in Figure (6) and Figure (7).
- 2- Positioning the test specimen to be concentric with the loading plates and the loading center.



I Press platens. II Lining plates with grooves to prevent slippage. III Deflection gauges.
Figure (6): Sketch for the Setup of the Compression Test.





Figure (7): Specimen while being tested.

Level 1, The maximum load, as specified in 4.3.3.1. (218.75 ton) shall be applied to the bearing, held for 1 min and then removed. This process shall be repeated so that two complete loading and unloading cycles are carried out.

After a further 10 min under zero load, the deflection gauges shall be re-zeroed at a load corresponding to 5 MPa and then the load shall be applied progressively with a minimum of six increments. At each measuring point, the load shall be maintained at a constant value for a minimum of 2 min to minimise viscoelastic effects. When the bearing is fully loaded a visual examination of the exposed surfaces shall be made.

NOTE 1 Initial deflection may be disproportionately large as a result of bedding down.

NOTE 2 Additional information may be obtained, if required, about the viscoelastic behaviour of the elastomer at maximum load, by maintaining the load and observing the resulting creep over a period of 30 min.

Level 2, The maximum compressive load shall be applied to the bearing and released before any measurements are taken.

After this first loading, the maximum compressive load, as specified in 4.3.3.2 shall be applied progressively with a minimum of five increments at a rate of $5 \pm 0,5$ MPa / min.

The deflection shall be recorded at 1/3 of the maximum load and at the maximum load. A visual examination of the exposed surfaces shall be made.

Level 3, The maximum compressive load, as specified in 4.3.3.3 shall be applied and a visual examination of the exposed surfaces of the bearing shall be made. Removing the load gradually while recording the corresponding deformation measurements.

Test Results

- Figure (8): Shows the relationship between the load and the vertical deformation (Shortening) for each one of the four LVDTs during the third loading cycle.

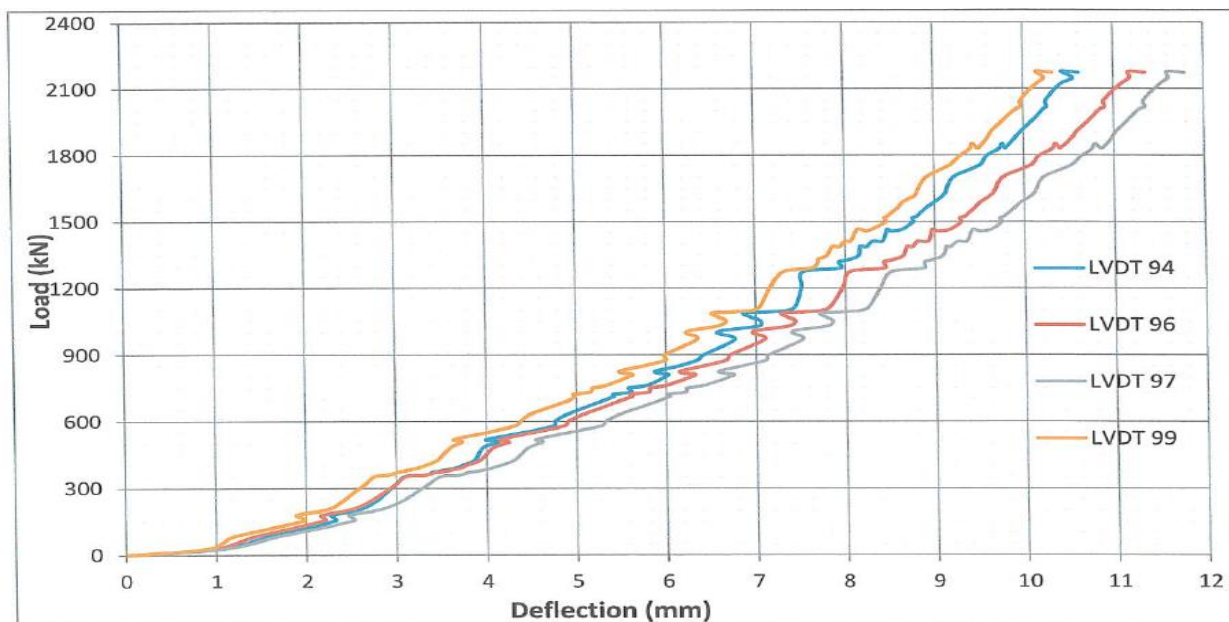


Figure (8): Load-Deformation relationship for specimen B3 during third loading cycle (Results obtained from the 4 LVDTs simultaneously).

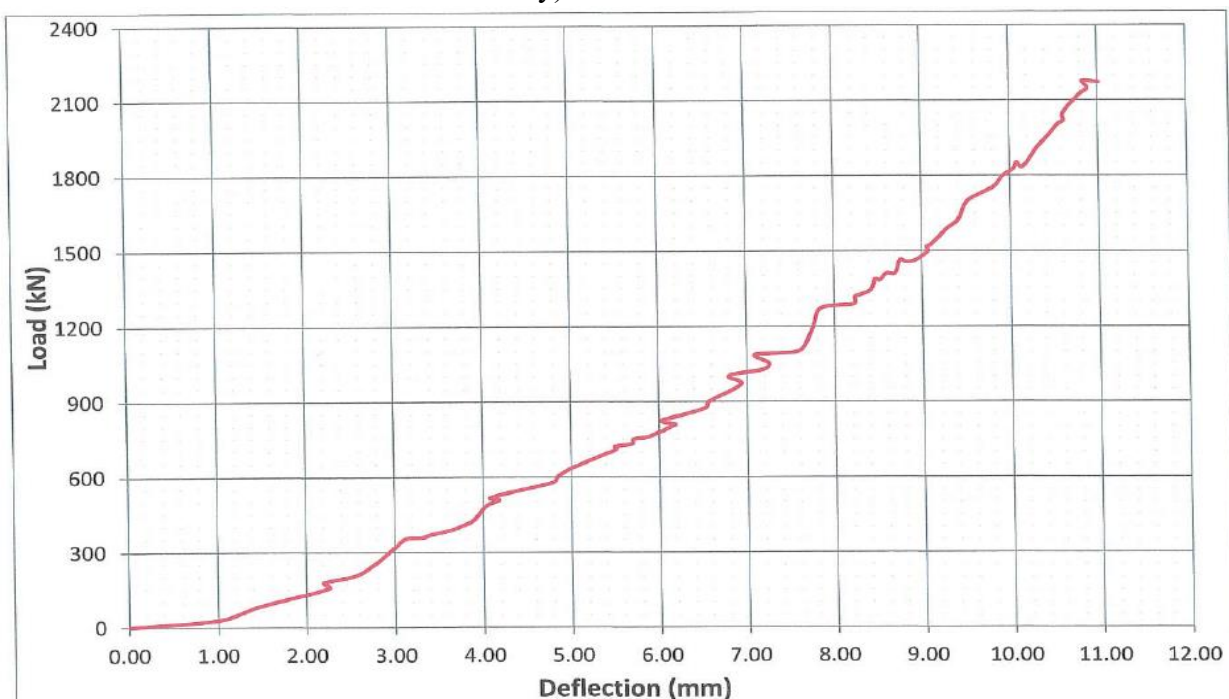


Figure (9): Load-Deformation relationship for specimen B3 during third loading cycle (Average displacement resulting from averaging values from the 4 LVDTs).

Modulus of Elasticity Calculation

Compressive strain (Levels 1 and 2), The results obtained from the third loading cycle were used to determine the modulus elasticity for the specimens as per the following equations:



The compressive strain, ε_c , is given by:

$$\varepsilon_c = \frac{v_z}{T_o} \quad (4)$$

where, v_z is the average recorded deflection and T_o , is the average total initial thickness of rubber ignoring the top and bottom covers.

$$\varepsilon_{c1}(@72.9ton) = \frac{7.12}{72} = 0.0989 \quad (5)$$

$$\varepsilon_{c2}(@218.75ton) = \frac{12.23}{72} = 0.170 \quad (6)$$

NOTE The value of the deflection between zero load and the first value recorded should be obtained by linear extrapolation.

Intersecting compression modulus (Level 1), If the compressive load (F2) is measured in Newtons, and the lengths in mm, then the compressive modulus will be given in MPa.

$$E_{cs} = \frac{\sigma_{c2} - \sigma_{c1}}{\varepsilon_{c2} - \varepsilon_{c1}} \quad (7)$$

where σ_{c2} is the stress at maximum load, σ_{c1} is the stress at 1/3 maximum load, ε_{c2} is the strain at maximum load and ε_{c1} is the strain at 1/3 maximum load.

$$\sigma_{c1}(@72.9ton) = \frac{729000}{350 \times 450} = 4.629 \quad (8)$$

$$\sigma_{c1}(@218.75ton) = \frac{2187500}{350 \times 450} = 13.889 \quad (9)$$

$$E_{cs} = \frac{13.889 - 4.629}{0.170 - 0.0989} = 130.24 \text{ MPa} \quad (10)$$

Compressive Stiffness calculations

The compression stiffness of high-damping rubber bearings is determined according to the method specified in this paper.

For the type test, level 1 of the compressive test method is applicable.

For the routine test, level 2 of the compressive test method is applicable.

For a particular project, when specified by the structure designer, level 3 of the compressive test method is applicable.

The results obtained from the third loading cycle were used to determine the compressive stiffness of the specimens as per the following equations:

$$C_c = \frac{F_{z2} - F_{z1}}{V_{z2} - V_{z1}} \quad (11)$$

where:

- F_{z2} and F_{z1} are respectively the maximum load and 1/3 load of the maximum load
- $V_{z2} - V_{z1}$ are the corresponding vertical deflection of the bearing at the same two loads



$$C_s = \frac{2187.5 - 729}{12.23 - 7.12} = 285.42 \text{ KN/mm} \quad (12)$$

If the compressive load (F_z) is measured in Newtons, and the lengths in mm, then the compressive modulus will be given in MPa.

Visual examination

Any surface defects or irregular surface corrugations which would indicate irregularly positioned plates or irregular bulges which would indicate bond failures near the surface shall be recorded.

Summary and conclusions

This paper presents a system of high-damping rubber bearings (HDRB) that is particularly suitable for near-fault areas where the pulsation effect in ground motions can exist. The study began with an experimental investigation on HDRB samples, and their hysteretic and ultimate behavior were studied. The value of the deflection between zero load and the first value recorded should be obtained by linear extrapolation. The initial deflection may be disproportionately large as a result of bedding down. Additional information may be obtained, if required, about the viscoelastic behaviour of the elastomer at maximum load by maintaining the load and observing the resulting creep over a period of 30 min.

The seismic response of a Russky cable-stayed bridge with a high-damping rubber bearing (HDRB) isolation system was studied. The better performance of the HDRB with a higher amount of damping suggests the possible use of supplemental damping devices along with seismic isolators for improving the seismic performance of cable-stayed bridges.

In terms of vertical stiffness, the results from different loading cases show that HDRB possesses a better vertical isolation effect, better environmental protection, greater bearing capacity, and, similarly, a more environmentally friendly property. A corrected calculation of the vertical stiffness of the bearing is proposed based on the results of the study. The results show that HDRB has stable and reliable performance in rubber insulation systems among all types of bearings. Its vertical stiffness can be accurately calculated through the proposed modified equation.

All experimental data found that the proposed corrected equation can calculate the vertical stiffness of bearings with higher accuracy. This paper presents the results of an experimental study aimed at further exploring the concepts of low-form, high-damping rubber bearings applied in seismic isolation of cable-stayed bridges.

Hence, it can avoid the unfavorable resonance effect caused by vertical periodic coupling within the structure. All the experimental data show that the proposed corrected equation can calculate the vertical stiffness of bearings with higher accuracy. This paper presents the results of an analytical, parametric study that aimed to further explore the low-shape factor concepts of rubber bearings applied in three-dimensional isolation for building structures.



Based on the investigation performed on the seismic response control of the bridge, the following conclusions are drawn:

- In spite of being a flexible structure, a cable-stayed bridge can achieve a significant reduction in the seismic response of the bridge by installing an HDRB. The acceleration and basic shear response can be reduced slightly with the HDRB insulation system, but at the expense of the large displacement response of the deck.
- The reduction of seismic responses depends on the types of insulation as well as the types of seismic ground motions.
- Increasing the damping ratio of HDRB, reduces the seismically induced forces of the bridge. On the other hand, the time period of insulation of insulators has a significant impact on seismic responses but again depends on the types of earthquake ground motion.
- It can be concluded that HDRB is more powerful and has better performance than some other insulators.
- In the experimental test, the resulting values of vertical deflection from the compression test method were on the safe side.

Data Availability Statement All data, models, and code generated or used during the study appear in the submitted article.

Funding: The authors declare that no funding or other support were received during the preparation of manuscript.

Declarations Conflict of Interest On behalf of all authors, the corresponding author states that there is no conflict of interest.

References

1. Casciati, F., Cimellaro, G. P., & Domaneschi, M. (2008). Seismic reliability of a cable-stayed bridge retrofitted with hysteretic devices. *Computers & Structures*, 86(17-18), 1769-1781.
2. Ren, W. X., & Obata, M. (1999). Elastic-plastic seismic behavior of long span cable-stayed bridges. *Journal of Bridge Engineering*, 4(3), 194-203.
3. Ahmed, A. R., & Ermoshin, N. (2022, May). Assessment of the Cable-Stayed and Cable Damping System Used in the Russky Bridge and Determination of the Force Acting on the Bridge's Cables. In *International Scientific Conference on Agricultural Machinery Industry "Interagromash"* (pp. 2719-2730). Cham: Springer International Publishing.
4. Chang, K. C., Mo, Y. L., Chen, C. C., Lai, L. A. C., & Chou, C. C. (2004). Lessons learned from the damaged Chi-Lu cable-stayed bridge. *Journal of Bridge Engineering*, 9(4), 343-352.
5. Ali, H. E. M., & Abdel-Ghaffar, A. M. (1994). Seismic energy dissipation for cable-stayed bridges using passive devices. *Earthquake engineering & structural dynamics*, 23(8), 877-893.



6. Li, H., Liu, J., & Ou, J. (2011). Seismic response control of a cable-stayed bridge using negative stiffness dampers. *Structural Control and Health Monitoring*, 18(3), 265-288.
7. Martínez-Rodrigo, M. D., & Filiatrault, A. (2015). A case study on the application of passive control and seismic isolation techniques to cable-stayed bridges: A comparative investigation through non-linear dynamic analyses. *Engineering Structures*, 99, 232-252.
8. Shrestha, B. (2015). Seismic response of long span cable-stayed bridge to near-fault vertical ground motions. *KSCE Journal of Civil Engineering*, 19, 180-187.
9. Wang, J., Zou, X., Yan, X., & Li, S. (2015). Integrated analysis model for the seismic responses of cable-stayed bridges near active faults. *Journal of Earthquake and Tsunami*, 9(01), 1550002.
10. Li, S., Dezfali, F. H., Wang, J. Q., & Alam, M. S. (2018). Longitudinal seismic response control of long-span cable-stayed bridges using shape memory alloy wire-based lead rubber bearings under near-fault records. *Journal of Intelligent Material Systems and Structures*, 29(5), 703-728.
11. Gu, Z., Lei, Y., Qian, W., Xiang, Z., Hao, F., & Wang, Y. (2021). An experimental study on the mechanical properties of a high damping rubber bearing with low shape factor. *Applied Sciences*, 11(21), 10059.
12. Ahmed, A. R., & Yermoshin, N. A. (2024). Optimum design of cable-stayed bridges considering cable loss scenarios. *Asian Journal of Civil Engineering*, 25(3), 2801-2809.
13. Pipinato, A. (2016). Case study: the Russky bridge. In *Innovative bridge design handbook* (pp. 671-680). Butterworth-Heinemann.
14. Ahmed, A. R., & Ermoshin, N. (2022). Method for investigating the reliability of structural elements of cable-stayed supports' anchorage: a case study of the Russky Bridge. *Transportation Research Procedia*, 63, 2887-2897.
15. Soneji, B. B., & Jangid, R. S. (2006). Effectiveness of seismic isolation for cable-stayed bridges. *International Journal of Structural Stability and Dynamics*, 6(01), 77-96.
16. Fang, C., Liang, D., Zheng, Y., & Lu, S. (2022). Seismic performance of bridges with novel SMA cable-restrained high damping rubber bearings against near-fault ground motions. *Earthquake Engineering & Structural Dynamics*, 51(1), 44-65.